2011

Reduction of Benzylidene Dibenzo[a, d]cycloheptenes: Over-Reduction of Antiaromatic Dianions to Aromatic Tetraanions

Blakely Tresca
Trinity University

MacDonald Higbee
Trinity University

Nancy S. Mills
Trinity University, nmills@trinity.edu

Repository Citation

Tresca, B., Higbee, M., & Mills, N. S. (2011). Reduction of benzylidene dibenzo[a, d]cycloheptenes: Over-reduction of antiaromatic dianions to aromatic tetraanions. *Journal of Organic Chemistry, 76*(14), 5539-5546. doi:10.1021/jo200227t

JOC The Journal of Organic Chemistry

ARTICLE

pubs.acs.org/joc

Reduction of Benzylidene Dibenzo[*a*,*d*]cycloheptenes: Over-Reduction of Antiaromatic Dianions to Aromatic Tetraanions

Blakely Tresca, MacDonald Higbee, and Nancy S. Mills*

Department of Chemistry, Trinity University, San Antonio, Texas 78212-7200, United States

Supporting Information

ABSTRACT: The antiaromaticity of a series of dianions of *p*-substituted benzylidene dibenzo[*a*,*d*]cycloheptenes was examined through calculated measures of antiaromaticity. The nucleus-independent chemical shifts (NICS) and magnetic susceptibility exaltation both showed substantial antiaromatic character in the benzannulated tropylium anion. When the antiaromaticity was normalized for the area of the ring, these tropylium anions were shown to be among the most antiaromatic anions in the chemical literature. Attempts to make the dianion through reduction with lithium or potassium gave the tetraanion as the only species observable in the ^{1}H NMR spectrum. Quench of the reaction mixture with trimethylsilyl chloride or D_2O confirmed the presence of the tetraanion, but only as a small portion of the reaction mixture, with the major product being unreacted starting material. The failure to observe starting material was attributed to similarities in the structures of the starting material and anion radical (first reduction), allowing rapid electron transfer between them. The inability to see the dianion (second reduction) could be the result of the very small HOMO−LUMO gap anticipated for highly antiaromatic species, which would allow access to diradical species. The magnitude of the HOMO−LUMO gap was determined by the difference between the HOMO and LUMO energies from geometry optimization and the lowest energy transition from TD-DFT calculations. The HOMO−LUMO gap for the benzylidene dibenzocycloheptatriene dianions was shown to be much smaller than the HOMO−LUMO gap of species for which ^{1}H NMR spectra had been observed.

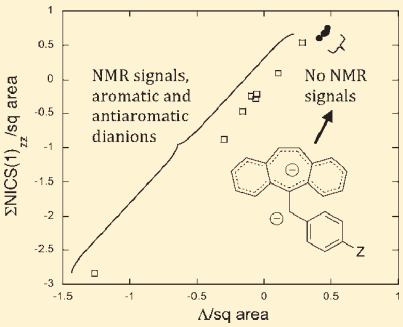

INTRODUCTION

Aromaticity has occupied a central role in organic chemistry because the stability associated with the aromatic sextet has dictated the formation of products from a wide variety of reactions. Interest in the aromatic sextet and related expansion to other species with a Hückel number of electrons in a conjugated π-system led to the development of a number of nonbenzenoid aromatic species. These species were determined to be aromatic based on a number of properties associated with benzene. Their stability was evaluated through *energetic* measures, such as aromatic stabilization energy,[1] through *structural* measures, such as planarity and lack of bond length alternation,[2] and through *magnetic* measures, such as the diatropic shift of protons on the periphery of the ring system,[3] nucleus-independent chemical shifts (NICS),[4,5] and magnetic susceptibility exaltation.[6]

Much less attention has been paid to the preparation of antiaromatic systems because of their anticipated instability. We have been able to prepare and characterize experimentally a number of antiaromatic dications of fluorenyl systems[7−11] and have extended those studies to antiaromatic indenylidene dications.[12,13] More recently, we have prepared antiaromatic dianions containing dibenzotropylium anions[14] as well as those containing heterocyclic antiaromatic systems such as the dianion of dixanthyidene.[15]

Herein we report the attempt to prepare and characterize dianions of substituted benzylidene dibenzocycloheptenes (**1**) through reduction with lithium or potassium. We anticipated that the electron-donating (destabilizing) group on the benzyl substituent would enhance the antiaromaticity of the dibenzotropylium anion just as electron-withdrawing groups on the benzyl substituent of the analogous benzylidene fluorene dications had enhanced the antiaromaticity of the fluorenyl system.[7] We observed instead the over-reduction of the desired dianion ($\mathbf{1}^{2-}$) to an unexpected tetraanion ($\mathbf{1}^{4-}$), which contains an aromatic dibenzotropylium trianion (Scheme 1). Of particular interest was our inability to observe the dianion in the ^{1}H NMR spectrum of the reaction mixture. There are two possibilities for this result: that the dianion was sufficiently unstable that it was immediately reduced to the tetraanion or that the antiaromatic dianion had a sufficiently small HOMO/LUMO gap to give the dianion appreciable diradical character. The presence of the tetraanion is confirmed through comparison of its experimental and calculated chemical shifts and through mass spectral data of its quench products. The evidence for the small HOMO/LUMO gap comes from the $\Delta E_{HOMO}-E_{LUMO}$ from the geometry optimization and from the lowest energy electronic transition from TD-DFT calculations.

Received: January 30, 2011
Published: May 24, 2011

Scheme 1. Reduction of 1

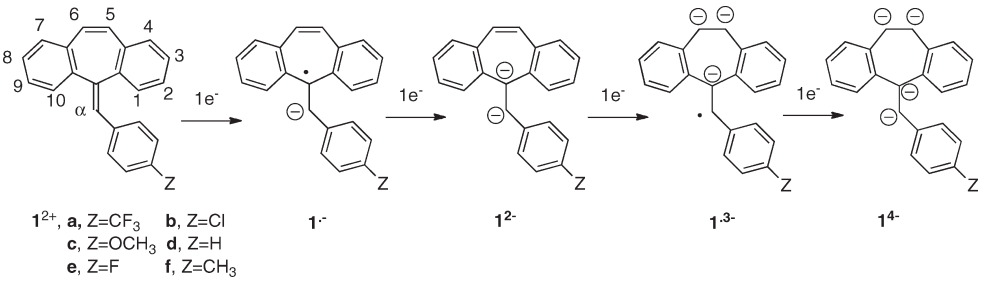

Table 1. Nucleus-Independent Chemical Shifts, NICS(1)$_{zz}$[a], for 1a^{2-}−1f^{2-}

	NICS(1)$_{zz}$, 7-ring, ppm	NICS(1)$_{zz}$, 6- ring, ppm	ΣNICS(1)$_{zz}$ for all rings, ppm	ΣNICS(1)$_{zz}$/area^2, ppm/Å^2
1a^{2-}	108.02	42.41	192.85	0.609
1b^{2-}	115.79	48.56	212.92	0.668
1c^{2-}	116.74	49.51	215.77	0.677
1d^{2-}	118.62	51.29	221.21	0.694
1e^{2-}	118.40	51.46	221.32	0.695
1f^{2-}	125.91	56.72	239.35	0.751

[a] Shifts calculated with the GIAO method with basis set B3LYP/6-311+G(d,p) on geometries optimized at the B3LYP/6-31G(d) level. Ghost atom placed 1 Å above the ring. NICS evaluated using only the component of the magnetic tensor parallel to the π-system.[17]

RESULTS AND DISCUSSION

Calculated Measures of Antiaromaticity for 1^{2-}. *Nucleus-Independent Chemical Shifts.* The ring current model of aromaticity predicts a magnetic environment in the center of an aromatic ring that is opposite in sign to that of the periphery, resulting in protons that are shifted downfield when on the periphery of an aromatic species and would be shifted upfield if present in the center of the aromatic ring. These effects would be opposite for an antiaromatic species, and these predictions have been given experimental support in the ^{1}H NMR characterization of [18]annulene and its dianion.[16] Nucleus-independent chemical shifts, NICS, are based on this phenomenon, with the calculation of the magnetic shielding tensor for a ghost atom placed in the center of the ring system.[4] NICS for an aromatic system have a negative sign; those for an antiaromatic system have a positive sign.

The calculated NICS(1)$_{zz}$ values for the dibenzotropylium systems of 1a^{2-}−1f^{2-} are given in Table 1. The positive values support the prediction of antiaromaticity in these anionic dibenzotropylium systems, with larger values indicating greater antiaromaticity. In general, electron-withdrawing substituents cause a decrease in the antiaromaticity due to the stabilization of the anionic system. The methoxy substituent is behaving more as an inductively withdrawing group than a resonance-donating group, as seen by the decreased antiaromaticity. The methyl-substituted dianion is the most antiaromatic system in the series.

Magnetic Susceptibility Exaltation. A second magnetic measure of aromaticity and antiaromaticity arises from the additional response to a magnetic field of a species with a ring current. This additional magnetic susceptibility is called magnetic susceptibility exaltation, Λ.[6,18−21] The magnetic susceptibility, *X*, can be calculated with the CSGT (continuous set of gauge transformations) method for the entire species. This is then compared to the sum of the magnetic susceptibility for the individual bonds in the system, giving in essence the magnetic susceptibility for the nondelocalized system. The difference between the two susceptibility values is the exaltation due to the ring current (see Supporting Information for details of the calculations). As is true for NICS, a negative value of Λ is associated with aromatic systems and a positive value with antiaromatic systems. The calculated magnetic susceptibilities, *X*, of 1a^{2-}−1f^{2-} and the magnetic susceptibility exaltation Λ are given in Table 2. Comparison of the ΣNICS(1)$_{zz}$ and Λ shows similar trends in the effect of the substituent on the antiaromaticity of the dibenzotropylium anion. The magnitude of both Λ[6] and ΣNICS(1)$_{zz}$[22] is related to the square area of the system under examination. For similarly sized species such as 1a^{2-}−1f^{2-}, it is reasonable to compare the NICS and Λ values directly. However, to place these values in a larger context by comparison with other aromatic and antiaromatic species, each value needs to be normalized by the square area of the ring system. We have demonstrated a linear relationship between the ΣNICS(1)$_{zz}$/sq area and Λ/sq area,[22] and that relationship is shown in Figure 1,

Table 2. Magnetic Susceptibility[a], *X*, and Magnetic Susceptibility Exaltation, Λ, for 1a^{2-}−1f^{2-}

	X^b	Λ^b	Λ/area^2
1a^{2-}	−33.52	129.82	0.410
1b^{2-}	−17.23	141.58	0.444
1c^{2-}	−7.63	145.52	0.456
1d^{2-}	10.68	149.37	0.469
1e^{2-}	2.94	147.95	0.465
1f^{2-}	0.73	150.42	0.472

[a] Shifts calculated with the CSGT method with basis set B3LYP/6-311+G(d,p) on geometries optimized at the B3LYP/6-31G(d) level. See Supporting Information for details of the calculation. [b] csgt/ppm.

dx.doi.org/10.1021/jo200227t |J. Org. Chem. 2011, 76, 5539–5546

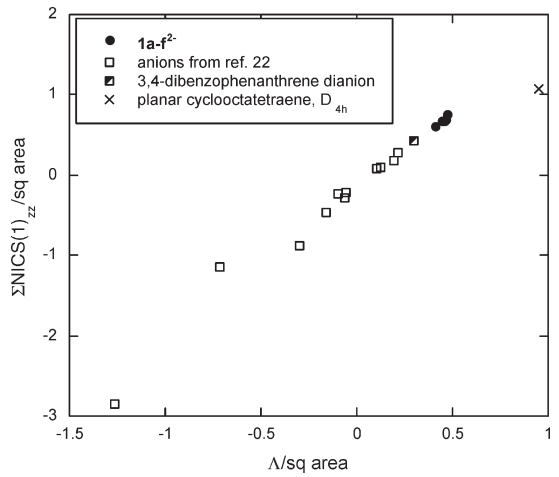

Figure 1. Relationship between $\Sigma NICS(1)_{zz}$/sq area and Λ/sq area for $\mathbf{1a}-\mathbf{f}^{2-}$ and a set of mono- and dianions,[22] 3,4-dibenzophenathrene dianion, and planar cyclooctatetraene, calculated as described in Tables 1 and 2.

which includes a set of representative anions from ref 22 (see Supporting Information). Notice that $\mathbf{1a}^{2-}-\mathbf{1f}^{2-}$ are the most antiaromatic anions in this group which includes the dianion of 3,4-dibenzophenanthrene, vide infra.[23] The plot also includes planar (D_{4h}) cyclooctatetraene, which is presumed to be the transition state for inversion of the tub-shaped geometry of cyclooctatetraene.[24]

Attempted Preparation of $\mathbf{1a}^{2-}-\mathbf{1f}^{2-}$ through Reduction with Lithium or Potassium. Benzylidene dibenzocycloheptatrienes **1b**−**f** were synthesized through reaction of a substituted phenyl Grignard reagent with dibenzosuberenone, followed by dehydration (Scheme 2). The trifluoromethyl substituted compound **1a** was prepared through reaction of the Wittig product from 1-bromo-4-trifluoromethylbenzene with dibenzosuberenone.

The reduction of neutral precursors **1a**−**f** with lithium and potassium was attempted according to the method of Rabinovitz and Scott[25] and monitored by ^{1}H NMR spectroscopy. Within 10 min of sonication, the solution turned brown, and all peaks disappeared, with no peaks visible until after one hour of sonication. The ^{1}H NMR spectrum of the reduction by lithium of **1d** after one hour is shown in Figure 2. The COSY spectrum of the reaction mixture as well as the spectra from reduction of **1b**, **e**, and **f** are given in the Supporting Information. Neither **1a** nor **1c** gave clean enough reduction products for identification of the species present.

We assumed that the reduction would take place by one electron transfers giving initially the anion radical followed by the antiaromatic dianion $\mathbf{1}^{2-}$, which would presumably exist as $\mathbf{Li_2}\mathbf{1}$, vide infra. We therefore assumed that the species present after one hour was the dianion since the anion radical would be invisible in the ^{1}H NMR spectrum due to broadening.[26] The linear correlation between the calculated and experimental shifts seen previously for antiaromatic dications and dianions[14] would support the identification of the dianion. However, the agreement was particularly poor for $\mathbf{Li_2}[\mathbf{1b,d}-\mathbf{f}]$ (Figure 3a) but substantially better for $\mathbf{Li_4}[\mathbf{1b,d}-\mathbf{f}]$ (Figure 3b). For both sets of data, the shifts were calculated with the inclusion of solvent using the polarization continuum method, PCM.[27] We have presented the data with the protons on the phenyl rings distinct from the benzylic protons and the protons on the dibenzotropylium rings in Figure 3. The relationship for the phenyl protons is fairly linear for both the dianions and tetraanions, as would be expected since in both systems the amount of charge would be basically the same. However, there is no correlation for the dibenzotropylium/benzylic protons in the dianion, with a reasonable correlation for the tetraanion, $R = 0.941$.

Scheme 2. Preparation of *p*-Substituted 1

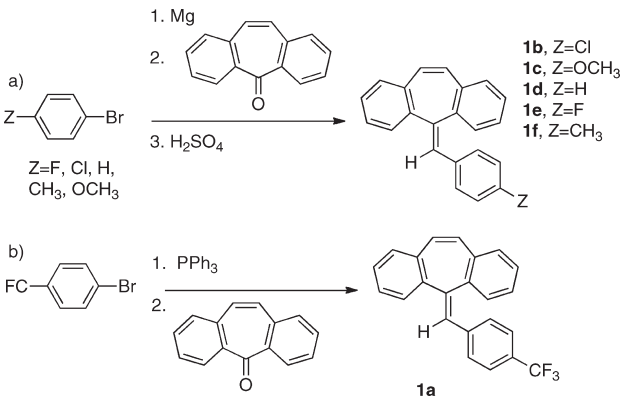

The experimental ^{1}H NMR chemical shifts and shifts calculated for $\mathbf{Li_4}[\mathbf{1b,d}-\mathbf{f}]$ are given in Table 3. The chemical shifts calculated for $\mathbf{Li_2}[\mathbf{1b,d}-\mathbf{f}]$ can be found in the Supporting Information. The proton assignments were made by a combination of COSY data and comparison with calculated shifts.

Identification of $\mathbf{Li_4}$1d in the Reaction Mixture. The reaction mixture after ~1 h of sonication was quenched with either $(CH_3)_3SiCl$ or D_2O in dry THF. Tetrasilylated or deuterated material was present in the reaction mixture, but it was only a small percentage of the silylated or deuterated material. Present in much larger concentration was unreacted starting material, followed by several trisilylated/deuterated products, then tetrasubstituted product, and disubstituted product (see Table 4). The ^{1}H NMR spectrum of the reaction mixture in Figure 2 clearly shows no unreacted starting material (see Supporting Information for the full spectrum) nor does it show substantial amounts of anything but $\mathbf{Li_4}\mathbf{1d}$. We did not anticipate seeing the mono- or trianion radicals in the spectrum of the reaction mixture, but the absence of spectral evidence for the starting material and dianion apparent from the quenches was of concern.

Spectral Invisibility of 1d in the Presence of an Anion Radical. The dominance of unreacted starting material in the mixture of products from quench with $(CH_3)_3SiCl$ or D_2O was of concern to us because it should have been apparent in the NMR spectrum of the reaction mixture. We considered the possibility of inadvertent quench of the anionic species by adventitious water but saw substantial amounts of starting material even with the most stringently anhydrous conditions. A possible explanation is based on in the changes seen in the ^{1}H NMR spectrum during reduction of cyclooctatetrane, COT, to the dianion with lithium or potassium.[28] The electron transfer between the anion radical and dianion of COT was rapid, resulting in broadening of the NMR signal, with the singlet of the dianion becoming sharp when two equivalents of metal were consumed. That is, while both anion radical and dianion existed in solution, the signal was broad. The spectrum of unreacted COT remained sharp until it was consumed. The explanation for the differing behavior of the two diamagnetic species involved

dx.doi.org/10.1021/jo200227t |J. Org. Chem. 2011, 76, 5539–5546

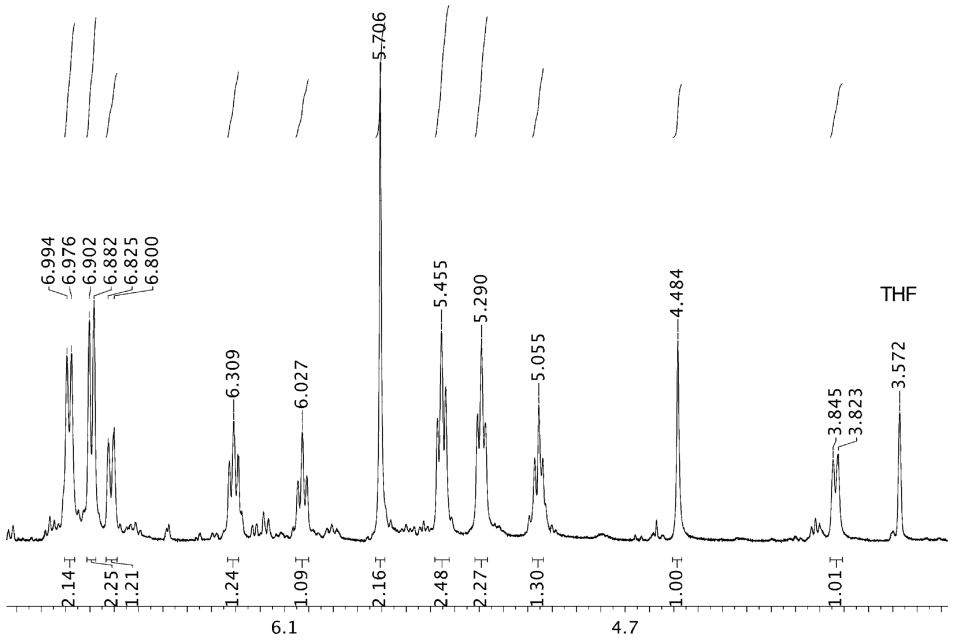

Figure 2. ^{1}H NMR spectrum of the reaction mixture from reduction of **1d** with lithium. TMS as reference. Peak at δ3.57 ppm due to residual THF-d_7.

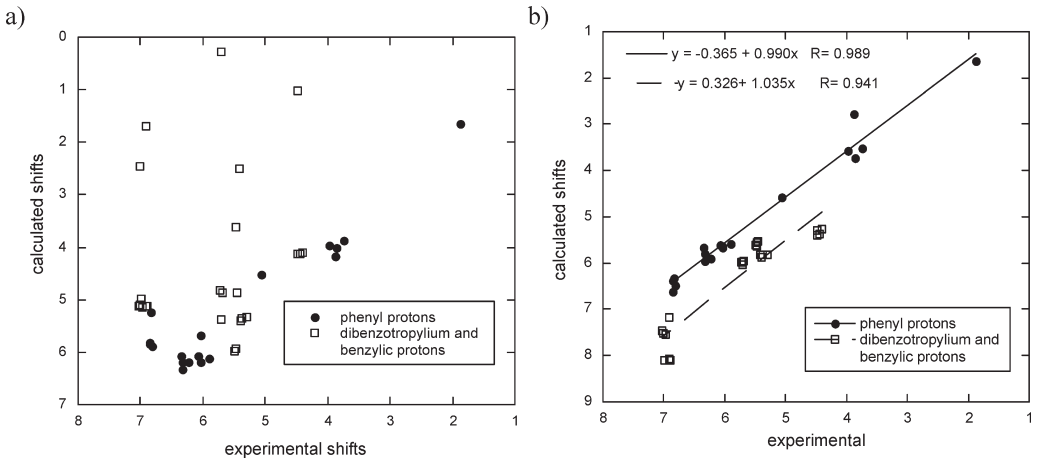

Figure 3. Comparison of experimental ^{1}H NMR chemical shifts from reduction of **1b**,**d**−**f** with shifts. Solvent was included in the calculations through use of the polarization continuum method, PCM. (a) **$Li_2$1b**,**d**−**f**. (b) **$Li_4$1b**,**d**−**f**.

their geometry. Neutral COT is tub-shaped, while the COT dianion is planar. Because electron transfer between two species with similar geometries is rapid, the broadening of the signal of the COT dianion suggested that the anion radical must also be planar. We have calculated the geometries of **1** and $\mathbf{1}^{\bullet-}$, and they are very similar and different from the geometry of **$Li_4$1** (see Figure 4 for **1** and $\mathbf{1}^{\bullet-}$ and Supporting Information). Thus, electron transfer between **1** and $\mathbf{1}^{\bullet-}$ would be expected to be rapid, resulting in broadening of the signal for starting material.

Spectral Invisibility of $Li_2$1d. Our inability to see any interpretable ^{1}H NMR signal during the reduction of **1d** until the formation of **$Li_4$1d** can be understood if the dianion was sufficiently antiaromatic that it possessed a very small HOMO−LUMO gap, allowing for diradial formation. The relationship between the HOMO−LUMO gap and aromaticity/antiaromaticity is based on stability. Molecules with large HOMO−LUMO gaps have been shown to be stable and unreactive; those with small HOMO−LUMO gaps have been shown to be chemically reactive.[29,30] The theoretical basis between the HOMO−LUMO gap and stability was articulated by Pearson, defined as hardness, η,[31] and considered as a measure of aromaticity.[32] Minsky et al.[33] and Shenhar[25] have reported the effect of a small HOMO−LUMO gap on the NMR spectra of a series of dianions of polycyclic aromatic hydrocarbons.

There are two methods for obtaining information about the HOMO−LUMO gap available through computation. The geometry optimization at an appropriate level provides the energies of the HOMO and LUMO. The energy for the first vertical excited state, from the HOMO to the LUMO, would approximate the HOMO−LUMO gap and can be calculated with time-

Table 3. Experimental[a] and Calculated[b] ^{1}H NMR Chemical Shifts for $Li_4$1b and Li_4[1d−f]

	$Li_4$1b		$Li_4$1d		$Li_4$1e		$Li_4$1f	
	exp.	calc.	exp.	calc.	exp.	calc.	exp.	calc.
1,10	6.91	7.186	6.99	8.093	6.91	8.100	6.888	8.086
2,9	5.50	5.602	5.46	5.542	5.47	5.560	5.461	5.650
3,8	5.37	5.829	5.39	5.878	5.41	5.815	5.294	5.827
4.7	6.98	7.541	7.02	7.475	7.01	7.527	6.999	7.530
5,6	5.68	5.965	5.71	6.027	5.71	5.973	5.714	5.991
α	4.45	5.380	4.49	5.284	4.49	5.265	4.401	5.399
o	6.85	6.388	6.82	6.478	6.83	6.627	6.844	6.320
o	3.98	3.579	3.85	3.727	3.87	3.512	3.730	2.778
m	6.34	5.658	6.33	5.956	6.32	5.890	6.232	5.799
m	6.07	5.604	6.04	5.653	6.04	5.596	5.887	5.632
p			5.06	4.577				
subst							1.877	1.6330

[a] Spectra in THF-d_8, temperature = 10 °C. [b] Chemical shifts calculated with the GIAO method with B3LYP/6-311+G(d,p) for geometries optimized at the B3LYP/6-31G(d) level; solvent (THF) included with the PCM method.

Table 4. Amounts of Di-, Tri-, and Tetrasilylated Product from $Li_4$1d,[a] from Reaction with Trimethylsilyl Chloride

	disilylated	trisilylated product-a	trisilylated product-b	trisilylated product-c	tetrasilylated product
percentage of all silylated product	4%	4%	22%	62%	8%

[a] From quench of a reduction mixture after 1 h of sonication. The ^{1}H NMR shifts for the reduction mixture correspond to those in Figure 2.

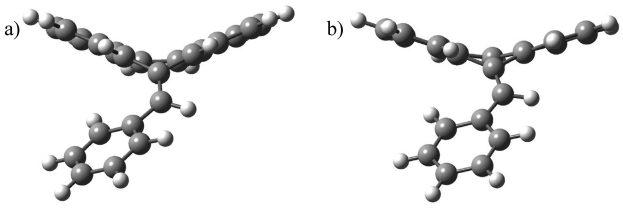

Figure 4. Calculated structures of **1d** and its monoanion radical. (a) Starting material (**1d**). (b) First reduction product.

dependent density functional theory, TD-DFT. We have demonstrated a good relationship between the experimental and calculated electronic spectra for antiaromatic dications.[34] The challenge for the calculation of properties of anions comes from several issues. While DFT methods are generally very good for larger molecular systems, questions have been raised about their use for anions because of a self-interaction error in approximate functionals.[35,36] The result is that the HOMO energy is positive, even for stable anions, indicating that a valence electron is unbound. A possible solution to this problem lies in the use of a long-range corrected version of the B3LYP functional.[37] We have determined that the geometries calculated for $\mathbf{1a}^{2-}$−$\mathbf{1f}^{2-}$ using B3LYP/6-31g(d) and the long-range corrected functional LC-BLYP/6-31+g(d) give HOMO−LUMO gap energies that demonstrate the same relative changes in $\mathbf{1a}^{2-}$−$\mathbf{1f}^{2-}$. That is, the changes in the HOMO−LUMO gap caused by different substituents on the phenyl ring vary in an analogous way for each type of optimization (see Supporting Information). In addition, NICS(1)$_{zz}$ values calculated for the geometries obtained with the two methods also show a linear relationship (see Supporting Information for a complete discussion of dependence on basis set and functional). Thus, it is appropriate to use the geometries optimized at this lower level to obtain HOMO−LUMO energies as well as magnetic properties.

A more troublesome issue deals with the association of the counterion. Anions in solution are known to have close associations with their counterions, either as contact or solvent separated ion pairs. It is clear from the relationship of the calculated and experimental shifts for the tetraanions that they exist as Li_4[1a−f], although we have not determined whether these are contact or solvent separated ion pairs. Monolithiated benzocycloheptatrene is believed to exist as a contact ion pair, based on chemical shift changes as a function of changes in temperature and counterion.[38] While we cannot confirm that $\mathbf{1a}^{2-}$−$\mathbf{1f}^{2-}$ exist as Li_2[1a−f], it is reasonable to assume that this is the case. Thus, it would also be reasonable to expect that the properties of the lithiated species should be examined rather than those of the dianion. There are two primary problems. There are no reports in the literature for the determination of NICS values and Λ on lithiated species. Indeed, it is difficult to determine the appropriate manner to include both the counterion and ghost atom necessary for the evaluation of NICS and difficult to determine the appropriate reference system that would include the counterion for the calculation of Λ. These problems are more difficult when one also includes the molecules of THF providing solvation for the counterion. The calculations also become prohibitively expensive, particularly TD-DFT, as the molecules become more complicated.

However, the work of Rabinovitz et al.[25,39,40] has demonstrated that the magnitude of the HOMO−LUMO gap calculated on dianions without counterions explains changes in their NMR spectra. Since this is the question we are examining, we will use the same process. We have previously been able to obtain ^{1}H NMR spectra for antiaromatic dications and dianions, which suggests that their HOMO−LUMO gaps must have been sufficiently great to prohibit much diradical character. Three of those species are dication $\mathbf{2}^{2+}$[41] and dianions $\mathbf{3}^{2-}$[14] and $\mathbf{4}^{2-}$.[42] We also consider the HOMO−LUMO gap of the dianion of 3,4-dibenzophenathrene, $\mathbf{5}^{2-}$, to make a link to the previous work of Minsky et al.,[23] which describes the effect of the HOMO−LUMO gap on its NMR spectrum. The HOMO−LUMO gap calculated on geometries optimized at the B3LYP/6-31g(d) level for $\mathbf{1a}^{2-}$−$\mathbf{1f}^{2-}$ and $\mathbf{2}^{2+}$, $\mathbf{3}^{2-}$, $\mathbf{4}^{2-}$, and $\mathbf{5}^{2-}$ are reported in Table 5, along with the calculated energy for the first excited state for a subset of these species. The magnitude of the energies of $\Delta E_{HOMO}-E_{LUMO}$ and the lowest energy electronic transition demonstrate that the HOMO−LUMO gap is indeed smaller for $\mathbf{1a}^{2-}$−$\mathbf{1f}^{2-}$ than for antiaromatic $\mathbf{2}^{2+}$, $\mathbf{3}^{2-}$, and $\mathbf{4}^{2-}$, whose NMR spectra we have been able to determine. The reduction of 3,4-dibenzophenanthrene to $\mathbf{5}^{2-}$ with lithium, sodium, and potassium failed to give an NMR spectrum with observable ^{1}H and ^{13}C signals. This was attributed to a "large population of the excited triplet state with two unpaired electrons". This would be expected for a system with the very small HOMO−LUMO gap shown in Table 5.

It remains to link the HOMO−LUMO gap to the antiaromaticity of $\mathbf{1a}^{2-}$−$\mathbf{1f}^{2-}$. As Figure 1 shows, the substituted dianions of **1** are more antiaromatic than antiaromatic dianions we and

Table 5. $\Delta E_{HOMO}-E_{LUMO}$[a] and $E_{first\ excitation}$[b] for $\mathbf{1a}^{2-}-\mathbf{1f}^{2-}$ and $\mathbf{2}^{2+}$, $\mathbf{3}^{2-}$, $\mathbf{4}^{2-}$, and $\mathbf{5}^{2-}$

	$\mathbf{1a}^{2-}$	$\mathbf{1b}^{2-}$	$\mathbf{1c}^{2-}$	$\mathbf{1d}^{2-}$	$\mathbf{1e}^{2-}$	$\mathbf{1f}^{2-}$	$\mathbf{2}^{2+}$	$\mathbf{3}^{2-}$	$\mathbf{4}^{2-}$	$\mathbf{5}^{2-}$
$\Delta E_{HOMO}-E_{LUMO}$	1.584	1.412	1.196	s1.310	1.306	1.316	1.858	2.089	2.925	1.159
$E_{first\ excitation}$				0.679			0.951	0.983	1.492	

[a] Geometries optimized at B3LYP/6-31G(d). [b] Energies in eV calculated with B3LYP/6-31G(d) and the TD-DFT method, on geometries optimized at the B3LYP/6-31G(d) level.[34]

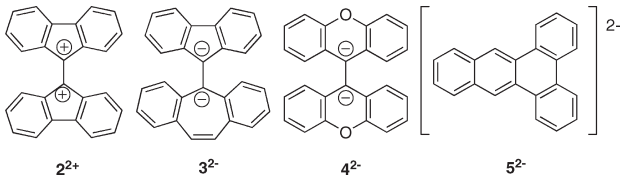

$\mathbf{2}^{2+}$ $\mathbf{3}^{2-}$ $\mathbf{4}^{2-}$ $\mathbf{5}^{2-}$

others have previously reported (see Supporting Information for the species represented in Figure 1). The NICS$(1)_{zz}$/square area and Λ/square area for $\mathbf{5}^{2-}$, whose lack of NMR signals supported the presence of a substantial triplet population, suggests that $\mathbf{1a}^{2-}-\mathbf{1f}^{2-}$ might also possess substantial diradical character. We will be examining the preparation of $\mathbf{1a}^{2-}-\mathbf{1f}^{2-}$ by deprotonation to allow evaluation of a diradical species and to characterize it as triplet vs singlet in a cleaner reaction medium.

SUMMARY

Dianions of **1** are among the most antiaromatic dianions reported in the literature, in terms of their NICS$(1)_{zz}$ and magnetic susceptibility exaltation, when normalized by the square of the ring area. Attempts to prepare the dianions by reduction with lithium or potassium resulted in over-reduction to tetraanions. Identification of the major species in the ^{1}H NMR spectrum of the reaction mixture as tetraanion was made through comparison of the calculated ^{1}H NMR shift of the tetraanion with the experimental spectrum. The relationship was substantially more linear than that of the calculated chemical shifts of the dianion with the experimental shifts. In both cases, comparison was made for chemical shifts calculated for the lithiated species in THF. However, quench of reaction mixtures which appear to contain only tetraanion with $(CH_3)_3SiCl$ or D_2O revealed that the major product was starting material, with evidence of mono-, di-, tri-, and tetrasubstituted product. The lack of NMR spectral evidence for unreacted starting material was rationalized through the similarity of the structures of starting material and mono-anion radical, leading to rapid electron transfer between the neutral and negative species. The lack of spectral evidence for dianion was rationalized by its apparent large antiaromaticity that would result in a small HOMO−LUMO gap, allowing for diradical character. The explanation was supported by a comparison of $\Delta E_{HOMO}-E_{LUMO}$ and by the lowest energy electron transition calculated by TD-DFT methods for $\mathbf{1}^{2-}$, with other antiaromatic dications and dianions, and by comparison to the behavior of the dianion of 3,4-dibenzophenathrene.

EXPERIMENTAL SECTION

Preparation of 1b−f. . The general procedure for formation of **1b**,[43] **1c**, **1d**,[43] **1e**,[44] and **1f** is shown below for the unsubstituted benzylidene dibenzocycloheptene **1d**.

5H-Benzylidene-dibenzo-(a,c)-cycloheptatriene, ***1d****.* Mg (16.5 mmol) was added to dry Et_2O (50 mL) and heated to reflux. Benzyl bromide (15.0 mmol) was dissolved in dry Et_2O (20 mL) and was added dropwise over 10 min to the refluxing flask. The flask was allowed to reflux for 2 h; the solution became metallic gray; and most of the Mg was consumed. Dibenzosuberenone (10.0 mmol) was dissolved in dry Et_2O (50 mL) and was added dropwise over 10 min to the refluxing flask. The reaction mixture was allowed to reflux for 2 h. The reaction was quenched with sat. aqueous NH_4Cl (25 mL) and then extracted with 2 × 10 mL of Et_2O. The combined organic layers were washed with 3 × 20 mL of water and then 3 × 20 mL of brine. The solvent was removed under vacuum to give a yellow oil. The yellow oil was dissolved in EtOH (20 mL), and H_2SO_4 in glacial acetic acid (20 mL, 20%) was added. The oil and acid were allowed to stir for 2 h, and then ice (50 mL) was added. The acid was neutralized with solid $NaHCO_3$, and the mixture was extracted with 3 × 20 mL of Et_2O. The combined organic layers were washed with 3 × 20 mL of sat. aqueous $NaHCO_3$, 3 × 20 mL of water, and 3 × 20 mL of brine. The solvent was removed under vacuum to give a yellow oil. Purification in a silica flash column with hexanes gave a white powder. Yield: 54%.

Melting Point and Spectral Data for 1c and 1f. **1c**, mp 93−97 °C. ^{1}H NMR (400 MHz, $CDCl_3$) δ 3.758 (s, 3H), 6.454 (s, 1H), 6.660 (dt, J = 9 Hz, 1 Hz, 2H), 6.894 (dt, J = 8.4 Hz, 1 Hz, 2H), 6.922 (d, J = 12 Hz), 6.986 (d, J = 12 Hz, 1 H), 7.139−7.331 (m, 5H), 7.374−7.454 (m, 2H), 7.526 (bd, J = 7.5 Hz, 1H). ^{13}C NMR (100 MHz, $CDCl_3$) δ 55.14, 113.30, 126.80, 126.93, 127.13, 128.29, 128.72, 128.83, 128.85, 129.13, 129.43, 130.38, 131.17, 131.44, 131.71, 134.38, 134.97, 137.69, 140.37, 142.79, 158.34. Calculated for $C_{23}H_{16}O$: C, 89.00; H, 5.85. Found: C, 88.82; H, 6.03.

1f, mp 112−114 °C. ^{1}H NMR (400 MHz, $CDCl_3$) δ 2.248 (s, 3H), 6.466 (s, 1H), 6.808 (d, J = 8.1 Hz, 1H), 6.917 (bd, J = 9.6, 2 H), 6.981 (d, J = 11.7H, 2 H), 7.109−7.222 (m, 2H), 7.257−7.315 (m, 3H), 7.361−7.461 (m, 2H), 7.520 (bd, J = 7.2 Hz, 1H). ^{13}C NMR (100 MHz, $CDCl_3$) δ 21.14, 126.87, 126.94, 127.15, 128.28, 128.58, 128.69, 128.78, 128.84, 129.08, 129.10, 131.19, 131.38, 132.20, 133.96, 134.33, 134.90, 136.46, 137.63, 141.40, 142.65 Calculated for $C_{23}H_{18}$: C, 93.84; H, 6.16. Found: C, 93.49; H, 6.24.

Preparation of Dianions. Benzylidene cycloheptatriene, **1** (10 mg, ~0.040 mmol), was added to a specially designed NMR tube insert (see Supporting Information) under Ar. Lithium wire (1 g, 150 mmol) was cleaned of oxide and mineral oil and added to the insert, followed by THF-d_8 (0.7 mL). The solution was degassed by freeze−pump−thaw and the insert flame-sealed under vacuum. The insert was inverted to bring the metal in contact with **1**, and reduction was initiated by sonication at 10 °C. Reduction appeared to begin after less than 5 min, with the development of a dark brown-orange solution. The products were monitored with NMR spectroscopy at 10 °C. The ^{1}H NMR spectra in Figure 2 and in the Supporting Information were taken after 1 h.

Quench Studies. Trimethylsilyl chloride (0.25 mL, 2.0 mmol) or D_2O (0.10 mL, 5.5 mmol) was added to dry THF (5 mL) and cooled to −78 °C in a septum capped flask. Previously prepared reduction samples were transferred to the quench solution with stirring, and the solution

was allowed to warm to room temperature. The solution changed from dark brown-orange to clear or pale yellow. The reaction mixture was neutralized with 10% HCl (2 mL); water (40 mL) was added. The solution was extracted with 3 × 10 mL of Et_2O, and the combined organic layers were washed with 2 × 10 mL of sat. aq. $NaHCO_3$. The solvent was removed under vacuum to give a white powder. The samples were purified with a silica plug with hexanes, and solvent was removed under vacuum. Solutions of the quench products in Et_2O (1%) were analyzed via GC/mass spectrometry (see Supporting Information for details and mass spectral data).

Computational Methods. Geometries were optimized at B3LYP/6-31G(d) density functional theory levels with the Gaussian 03 program package.[45] The chemical shifts were calculated at B3LYP/6-311+G(d,p) using the GIAO method on the geometries optimized with lithium counterions with the Gaussian 09 program.[46] The best agreement between experimental and calculated shifts was found when the effect of solvent was included in the calculation through the polarization continuum method, PCM, with the ε value of 7.4257, the default value for THF in Gaussian 03. The nucleus-independent chemical shifts $(NICS(1)_{zz})$[4,17] were obtained from the chemical shift tensor perpendicular to the ring for a ghost atom placed 1 Å above the center of each ring on geometries optimized without counterions. Magnetic susceptibility exaltation was determined from the magnetic susceptibility calculated for the substituted $\mathbf{1}^{2-}$ using the CSGT method with basis set B3LYP/6-311+G(d,p) by subtraction of the magnetic susceptibility for the localized system. Areas were calculated from the Cartesian coordinates for each ring system oriented in the *xy* plane. See Supporting Information for specific details of the calculation. TD-DFT calculations were done with the B3LYP/6-311+G(d,p) on the geometries optimized at the B3LYP/6-31G(d) level. See the Supporting Information for the discussion of the validity of geometry optimization with B3LYP/6-31G(d) vs that with functionals with long-range correction, such as LC-BLYP/6-31+G(d).

■ ASSOCIATED CONTENT

Supporting Information. Details on the calculation of magnetic susceptibility, ring areas, and Cartesean coordinates, frequencies, and energies of the optimized geometries of $\mathbf{1a}^{2-}$–$\mathbf{1f}^{2-}$, $\mathbf{Li_2}$[**1b**–**f**], with and without explicit THF, and $\mathbf{Li_4}$**1b** and $\mathbf{Li_4}$[**1d**–**f**], and $\mathbf{Li_4}$**1d**, with and without explicit THF, at varying levels of theory; ^{1}H NMR spectra of reduction of **1b**, **1d** (full spectrum), **1e**, and **1f**; ^{13}C NMR, COSY, and HMQC spectra of the reduction mixture of **1d**; calculated chemical shifts of dianions of $\mathbf{Li_4}$**1b** and $\mathbf{Li_4}$**1d**–**f**; mass spectra of the tetrasilylated product and tetradeuterated product; diagram of the insert used for reduction of **1**. This material is available free of charge via the Internet at http://pubs.acs.org.

■ AUTHOR INFORMATION

Corresponding Author
nmills@trinity.edu

■ ACKNOWLEDGMENT

We thank the Welch Foundation (Grant W-794), the National Science Foundation (Grants CHE-0126417, CHE-0553589, CHE-0957839, and CHE-0948445), and the Dr. John A. Burke, Jr. research fund for their support of this research and Dr. Cheryl Stevenson for helpful discussions.

■ REFERENCES

(1) Schleyer, P. v. R.; Puehlhofer, F. *Org. Lett.* **2002**, *4*, 2873–2876.
(2) Krygowski, T. M.; Cyranski, M. K. *Chem. Rev.* **2001**, *101*, 1385–1419.
(3) Mitchell, R. H. *Chem. Rev.* **2001**, *101*, 1301–1316.
(4) Schleyer, P. v. R.; Maerker, C.; Dransfeld, A.; Jiao, H.; Hommes, N. J. v. E. *J. Am. Chem. Soc.* **1996**, *118*, 6317–6318.
(5) Chen, Z.; Wannere, C. S.; Corminboeuf, C.; Puchta, R.; Schleyer, P. v. R. *Chem. Rev.* **2005**, *105*, 3842–3888.
(6) Gayoso, J.; Ouamerali, O. *Rev. Roum. Chim.* **1981**, *26*, 1035–1040.
(7) Do, C.; Hatfield, J.; Patel, S.; Vasudevan, D.; Tirla, C.; Mills, N. S. *J. Org. Chem.* **2011**, *76*, 181–187.
(8) Dahl, B. J.; Mills, N. S. *J. Am. Chem. Soc.* **2008**, *130*, 10179–10186.
(9) Dahl, B. J.; Mills, N. S. *Org. Lett.* **2008**, *10*, 5605–5608.
(10) Mills, N. S.; Benish, M. A. *J. Org. Chem.* **2006**, *71*, 2207–2213.
(11) Mills, N. S.; Tirla, C.; Benish, M. A.; Rakowitz, A. J.; Bebell, L. M.; Hurd, C. M. M.; Bria, A. L. M. *J. Org. Chem.* **2005**, *70*, 10709–10716.
(12) Mills, N. S.; Cheng, F. E.; Baylan, J. M.; Tirla, C.; Hartmann, J. L.; Patel, K. C.; Dahl, B. J.; McClintock, S. P. *J. Org. Chem.* **2011**, *76*, 645–653.
(13) Mills, N. S.; Llagostero, K. B.; Tirla, C.; Gordon, S.; Carpenetti, D. *J. Org. Chem.* **2006**, *71*, 7940–7946.
(14) Piekarski, A. M.; Mills, N. S.; Yousef, A. *J. Am. Chem. Soc.* **2008**, *130*, 14883–14890.
(15) Black, M.; Woodford, C.; Mills, N. S. *J. Org. Chem.* **2011**in revision.
(16) Oth, J. F. M.; Woo, E. P.; Sondheimer, F. *J. Am. Chem. Soc.* **1973**, *95*, 7337–7345.
(17) Fallah-Bagher-Shaidaei, H.; Wannere, C. S.; Corminboeuf, C.; Puchta, R.; Schleyer, P. v. R. *Org. Lett.* **2006**, *8*, 863–866.
(18) Haberditzl, W. *Angew. Chem., Int. Ed. Engl.* **1966**, *5*, 288–298.
(19) Dauben, H. J. J.; Wilson, D. J.; Laity, J. L. *J. Am. Chem. Soc.* **1968**, *90*, 811–813.
(20) Schmalz, T. G.; Norris, C. L.; Flygare, W. H. *J. Am. Chem. Soc.* **1973**, *95*, 7961–7967.
(21) Dauben, H. J.; Wilson, T. D.; L., L. In *Nonbenzenoid Aromaticity*; Snyder, J. P., Ed.; Academic Press: New York, 1971; Vol. 2, pp 167−180.
(22) Mills, N. S.; Llagostera, K. B. *J. Org. Chem.* **2007**, *72*, 9163–9169.
(23) Minsky, A.; Meyer, A. Y.; Poupko, R.; Rabinovitz, M. *J. Am. Chem. Soc.* **1983**, *105*, 2164–2172.
(24) Nishinaga, T.; Ohmae, T.; Iyoda, M. *Symmetry* **2010**, *2*, 76–97.
(25) Shenhar, R.; Beust, R.; Hagen, S.; Bronstein, H. E.; Willner, I.; Scott, L. T.; Rabinovitz, M. *J. Chem. Soc., Perkin Trans. 2* **2002**, 449–454.
(26) Sharp, R. R. *Nucl. Mag. Res.* **1995**, *24*, 469–513.
(27) Tomasi, J.; Mennucci, B.; Cammi, R. *Chem. Rev.* **2005**, *105*, 2999–3093.
(28) Katz, T. J. *J. Am. Chem. Soc.* **1960**, *82*, 3785–3786.
(29) Aihara, J. *J. Phys. Chem. A* **1999**, *103*, 7487–7495.
(30) Aihara, J. *Phys. Chem. Chem. Phys.* **1999**, *1*, 3193–3197.
(31) Pearson, R. G. *Acc. Chem. Res.* **1993**, *26*, 250–255.
(32) Zhou, Z.; Parr, R. G. *J. Am. Chem. Soc.* **1989**, *111*, 7371–7379.
(33) Minsky, A.; Meyer, A. Y.; Hafner, K.; Rabinovitz, M. *J. Am. Chem. Soc.* **1983**, *105*, 3975–3981.
(34) Mills, N. S.; Levy, A.; Plummer, B. F. *J. Org. Chem.* **2004**, *69*, 6623–6633.
(35) Roesch, N.; Trickey, S. B. *J. Chem. Phys.* **1997**, *106*, 8940–8941.
(36) Galbarith, J. M.; Schaefer, H. F., III *J. Chem. Phys.* **1996**, *105*, 862–864.
(37) Jensen, F. *J. Chem. Theory Comput.* **2010**, *6*, 2726–2735.
(38) Sethson, I.; Johnels, D.; Edlund, U. *Acta Chem. Scand.* **1990**, *44*, 1029–1031.
(39) Rabinovitz, M.; Ayalon, A. *Pure Appl. Chem.* **1993**, *65*, 111–118.
(40) Benshafrut, R.; Shabtai, E.; Rabinovitz, M.; Scott, L. T. *Eur. J. Org. Chem.* **2000**, 1091–1106.
(41) Mills, N. S. *J. Org. Chem.* **2002**, *67*, 7029–7036.
(42) Black, M.; Woodford, C.; Mills, N. S. *J. Org. Chem.* **2011**, *76*, 2286–2290.
(43) Bergmann, E. D.; Solomonovici, A. *Synthesis* **1970**, *2*, 183–189.

(44) Fox, H. H.; Gibas, J. T.; Lee, H. L.; Boris, A. *J. Med. Chem.* **1964**, *7*, 790–792.

(45) Frisch, M. J. T., G. W.; Schlegel, H. B.; Scuseria, G. E.; Robb, M. A.; Cheeseman, J. R.; Montgomery, J. A., Jr.; Vreven, T.; Kudin, K. N.; Burant, J. C.; Millam, J. M.; Iyengar, S. S.; Tomasi, J.; Barone, V.; Mennucci, B.; Cossi, M.; Scalmani, G.; Rega, N.; Petersson, G. A.; Nakatsuji, H.; Hada, M.; Ehara, M.; Toyota, K.; Fukuda, R.; Hasegawa, J.; Ishida, M.; Nakajima, T.; Honda, Y.; Kitao, O.; Nakai, H.; Klene, M.; Li, X.; Knox, J. E.; Hratchian, H. P.; Cross, J. B.; Bakken, V.; Adamo, C.; Jaramillo, J.; Gomperts, R.; Stratmann, R. E.; Yazyev, O.; Austin, A. J.; Cammi, R.; Pomelli, C.; Ochterski, J. W.; Ayala, P. Y.; Morokuma, K.; Voth, G. A.; Salvador, P.; Dannenberg, J. J.; Zakrzewski, V. G.; Dapprich, S.; Daniels, A. D.; Strain, M. C.; Farkas, O.; Malick, D. K.; Rabuck, A. D.; Raghavachari, K.; Foresman, J. B.; Ortiz, J. V.; Cui, Q.; Baboul, A. G.; Clifford, S.; Cioslowski, J.; Stefanov, B. B.; Liu, G.; Liashenko, A.; Piskorz, P.; Komaromi, I.; Martin, R. L.; Fox, D. J.; Keith, T.; Al-Laham, M. A.; Peng, C. Y.; Nanayakkara, A.; Challacombe, M.; Gill, P. M. W.; Johnson, B.; Chen, W.; Wong, M. W.; Gonzalez, C.; Pople, J. A. *Gaussian 03*, revision B.03 ed.; Gaussian, Inc.: Pittsburgh PA, 2004.

(46) R., A.; Frisch, M. J.; T., G. W.; Schlegel, H. B.; Scuseria, G. E.; Robb, M. A.; C., J. R.; Scalmani, G.; Barone, V.; Mennucci, B.; Petersson, G. A.; N., H.; Caricato, M.; Li, X.; Hratchian, H. P.; Izmaylov, A. F.; J. B., Zheng, G.; Sonnenberg, J. L.; Hada, M.; Ehara, M.; K. T.; Fukuda, R.; Hasegawa, J.; Ishida, M.; Nakajima, T.; Honda, Y.; K., O.; Nakai, H.; Vreven, T.; Montgomery, J. A., Jr.; Peralta, J. E.; O., F.; Bearpark, M.; Heyd, J. J.; Brothers, E.; Kudin, K. N.; S., V. N.; Kobayashi, R.; Normand, J.; Raghavachari, K.; R., A.; Burant, J. C.; Iyengar, S. S.; Tomasi, J.; Cossi, M.; R., N.; Millam, J. M.; Klene, M.; Knox, J. E.; Cross, J. B.; Bakken, V.; A., C.; Jaramillo, J.; Gomperts, R.; Stratmann, R. E.; Yazyev, O.; A. J. A.; Cammi, R.; Pomelli, C.; Ochterski, J. W.; Martin, R. L.; M., K.; Zakrzewski, V. G.; Voth, G. A.; Salvador, P.; D., J. J.; Dapprich, S.; Daniels, A. D.; Farkas, O.; F., J. B.; Ortiz, J. V.; Cioslowski, J.; Fox, D. J. *Gaussian 09*; Gaussian, Inc.: Wallingford CT, 2009.